

Diamond Strip Detectors for Charged Particle Tracking

Development of Novel Gas and Solid State Detectors

Joseph W. Tabeing (PI) and Valeriy V. Konovalov

Applied Diamond Inc., Wilmington, DE

Background and Motivation

To probe nuclei, scientists collide high-energy beams of electrons like those generated at CEBAF (JLAB) into atoms while studying protons, neutrons, quarks and gluons, the products of those collisions. A particular class of experiments makes use of parity violation in electron scattering to probe for new physics beyond the Standard Model, as well as explore the quark structure of nucleons. Such experiments require extremely precise knowledge of the electron beam polarization. In order to achieve acceptable precision, it is necessary to place the detector very close to the beam. Coupled with the expectation of long life-time and the potential for high current operation, the radiation dose seen by these detectors can approach 100 kGy for some experiments. At present, most radiation detectors are based on silicon technology, however, the practical radiation tolerance of silicon falls far short of requirements in future experiments and silicon must be cooled restricting the locations where it can be used. New radiation tolerant technologies must be developed to fill this gap and diamond has proven to be one such technology.

Diamond grown with chemical vapor deposition (CVD) has proven to be an excellent material for radiation detector applications. Diamond's large 5.6 eV band gap allows detectors with low leakage currents, its high electron and hole mobility ensures very fast signal response, its large lattice displacement energy and small cross section result in excellent radiation tolerance and its small dielectric constant provides low noise performance. Diamond's low atomic mass, long radiation length, high thermal conductivity, and low thermal expansion coefficient make it appropriate for high energy applications. Polycrystalline CVD (pCVD) diamond can be grown over large areas making it a good candidate material for these particle strip detectors.

In earlier projects, we successfully made high quality thin pCVD diamond films suitable for relativistic heavy ion applications and TOF measurements. For this project, thicker films were needed to provide increased signal, sufficient to overcome the additional noise inherent in placing electronics further from the detector.

Objectives vs Accomplishments

Phase I of this project accomplished its primary objectives of making thick film CVD diamond with acceptable charge collection properties by growing thick high purity material and then removing the small grain initial growth.

During the first year of Phase II, we were able to make several process refinements and to fabricate such a diamond sensor. During the second year of Phase II, process improvement continued, particularly in the area of diamond growth, defect removal, photolithography/metallization improvement, and detector packaging. We used several techniques to increase the CCD by 4 times that of our thin films. We developed a photolithography process to provide 200 μm wide electrical contacts with 25 μm gaps. We produced a strip detector with a sensor area of 48x12 mm and delivered it to JLAB for testing and use.

These results provide JLAB and other particle accelerator facilities with a material that will increase the lifetime of their particle detectors beyond that available from existing materials. In addition, a path forward now exists for making the large area diamond strip detectors needed for measuring electron beam polarization with Compton scattered electrons and other nuclear physics applications.

Project Activities

I. Improved Performance of Detector - Grade pCVD Diamond

a) Growth of High Quality Detector-Grade Diamond

We started by growing thin diamond wafers to optimize the diamond growth recipe and achieve high charge collection efficiency (CCE = CCD/Thickness). It has been suggested in the literature that the key factors for high CCE are high crystalline quality of diamond and its high purity. We found that CCE significantly depends on the diamond growth rate, see **Figure 1**, where slower growth gives better CCE results. Practically, we determined that the production of detector grade diamond with CCE $\approx 40\%$ requires a very slow growth rate of 0.3-0.4 $\mu\text{m/hr}$. We also investigated the dependence of CCE on the presence of the most common nitrogen impurity, characterized by the presence of the NV-center Raman peak, and confirmed that CCE drops at a high enough nitrogen level.

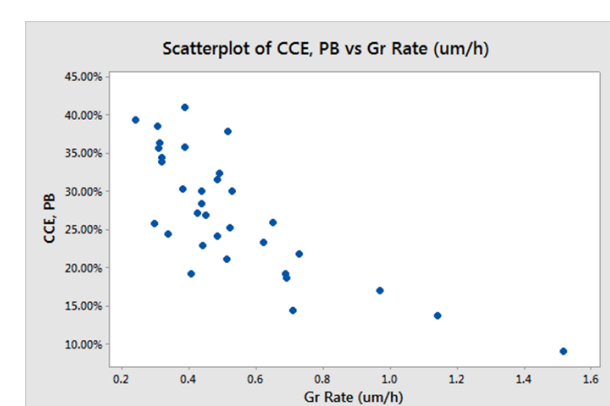


Figure 1. CCE (%) vs diamond growth rate ($\mu\text{m/hr}$).

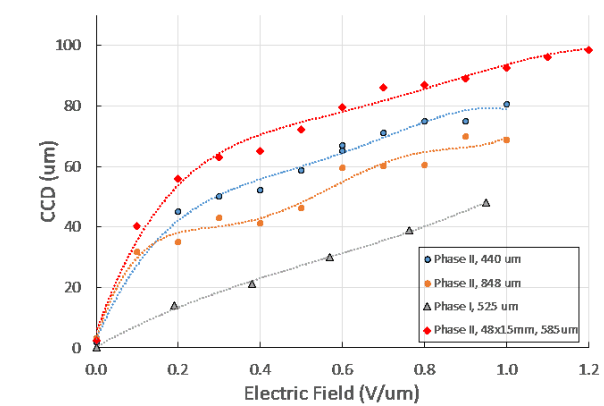


Figure 2. Charge collection distance for thick pCVD wafers grown with one reactor stop (Phase I), three stops (Phase II), three stops after back-thinning and after subsurface damage removal.

Next, we grew several 0.8 - 1.1 mm thick pCVD wafers using the same detector-grade recipe. The requirement of slow growth rate resulted in very long runs, e.g. for the 0.88 mm thick wafer it was 116 days. Unfortunately, 2-3 unscheduled shutdowns occurred during each long run due to a power outage, a cooling water problem, and a microwave generator failure. At each unexpected shutdown, wafers were given a thorough cleaning and in-situ plasma etching in the reactor. The wafer used for final detector fabrication showed 48% higher CCD than the wafer grown in Phase I and 67% higher after back-grinding, see **Figure 2**. Improvement also occurred after the subsurface polishing damage removal step discussed in Section C below.

b) Improvement of Charge Collection Uniformity

Uniformity of CCD across the diamond wafer depends upon the uniformity of diamond wafer thickness, crystalline uniformity and the distribution of defects. Two approaches were used to achieve improved thickness uniformity of the sensor: a) The growth chamber was equipped with a rotating holder to minimize the effects of plasma non-uniformity, see **Figure 3** and b) after a COMSOL thermal model was built, a new water-cooled stage geometry was designed that decreased the difference of 50°C measured before the change to 10°C, see **Figure 4**.

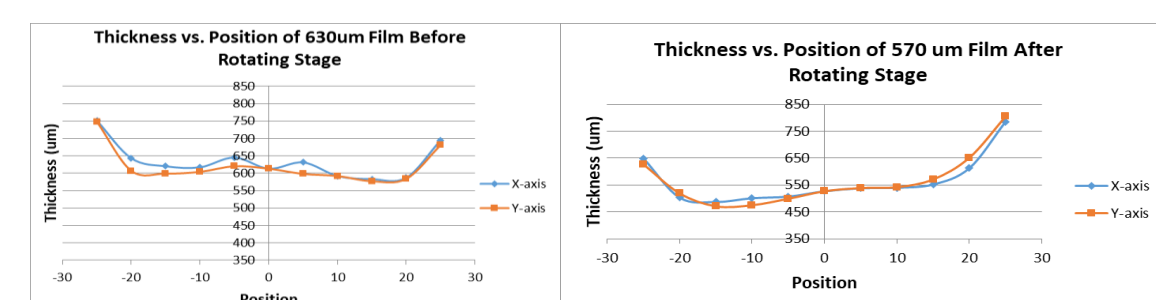


Figure 3. Thickness data from two wafers, without rotation and with rotation. The rotation did improve the central part of the wafer. The perimeter of the wafer, where the plasma couples to the holder, is often hotter than the center in this type of reactor resulting in thicker edges.

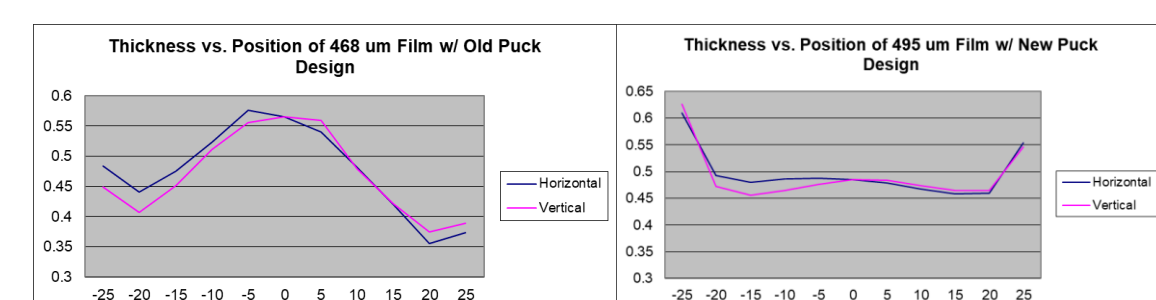


Figure 4. Thickness data from two wafers, one with the old "puck" design and with the new design, show the positive effect of temperature uniformity on thickness uniformity in the x and y-axis. Again, the perimeter of the wafer, where the plasma couples to the holder often produces a thick rim.

We also modified our CCD characterization setup to accommodate 2" wafers. **Figure 5** shows the maps of thickness and CCD, and demonstrates that we achieved about $\pm 10\%$ uniformity of thickness and CCD. We also found that the spatial distribution of CCD doesn't always correspond to the distribution of thickness.

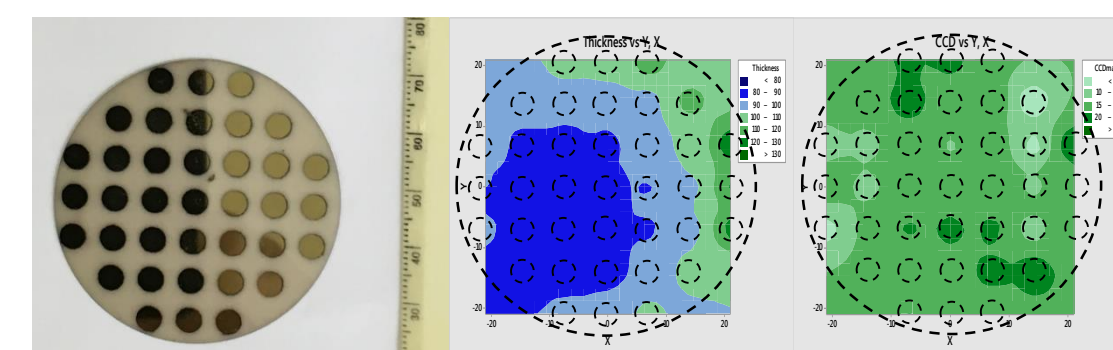


Figure 5. 2" diameter pCVD wafer with 82 μm average thickness (left), its thickness map (center) and CCD map (right). Each wafer was prepared for testing with 37 points (4 mm diameter Au/Cr contacts).

c) Study Material Removal vs. Improvement

The removal of material from the fine-grained substrate side of the diamond wafers increased CCD. Several 10 mm diameter disks were cut, see **Figure 12**, and initially polished from the growth side reducing the surface roughness from 30-60 μm to about 10-20 nm. Then they were polished from the substrate side to different thicknesses and for each thickness the disks were re-metallized and the CCD values measured again. **Figure 6** shows that CCE continuously increases with removal of small grain material from the substrate side, including the removal of the first damaged layer (created by the reactor's first unexpected stop) at about 218 μm from the substrate side. In addition, we applied a technique for removing polishing subsurface damage, presumably serving as charge carrier traps. **Figure 7** shows that a 15 - 20% improvement in CCD can be achieved this way. Finally, 35 - 45% CCE was achieved after removal of a significant part of the initial fine-grained material, including the complete removal of damaged layers, see **Figures 8, 9**.

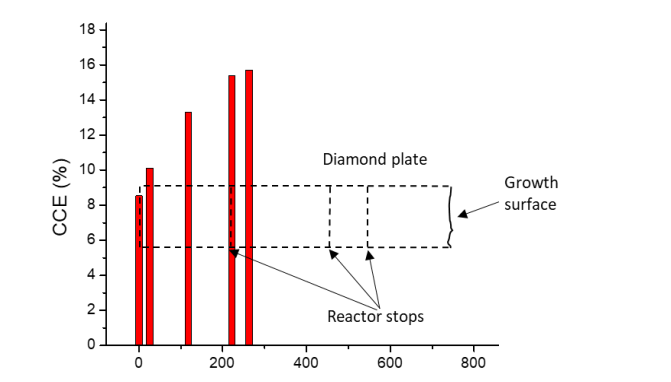


Figure 6. Charge collection efficiency (%) measured at different thicknesses of diamond plate (initial thickness 758 μm) after substrate side polishing. Diamond plate schematic shows the position of damaged layers resulted from three reactor stops.

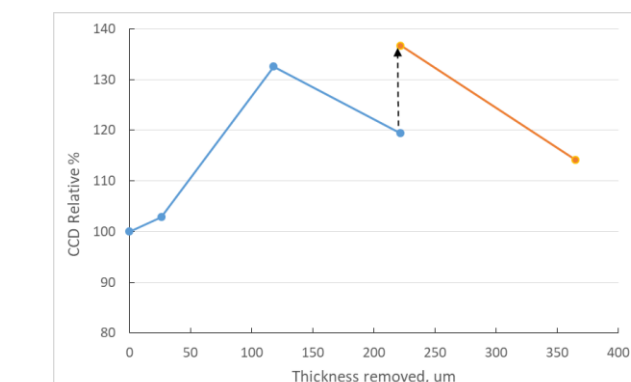


Figure 7. CCD improvement due to subsurface damage removal is shown by the break in the curve after 225 μm of material removal.

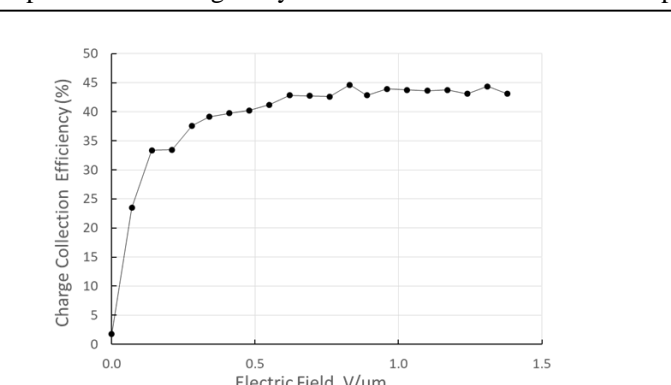


Figure 8. CCE of a 180 μm thick diamond layer laser cut close to the growth surface of about 900 μm thick wafer.

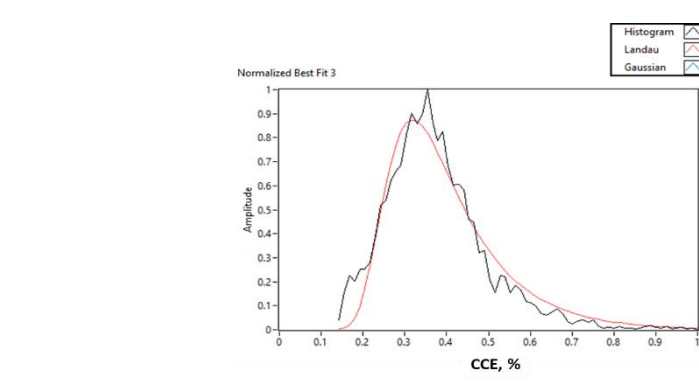


Figure 9. Normalized histogram of CCE (pulse height distribution) at electric field of 1.0 V/ μm for the diamond layer shown in Figure 8.

Conclusions:

- Detector quality thick polycrystalline CVD diamond films were developed. Several techniques were used to increase the charge collection result by 4 times that of our thin films. Photolithography processes were developed to provide 200 μm wide electrical contacts with 25 μm gaps. A diamond strip detector with a sensor area of 48x12x0.5 mm^3 and 192 metal strips (225 μm pitch) was fabricated and delivered to JLAB for testing and use.
- These results provide JLAB and other particle accelerator facilities with a radiation hard diamond material that will increase the lifetime of their particle detectors beyond that available from existing materials. In addition, a path forward now exists for making the large area diamond strip detectors needed for measuring electron beam polarization with Compton scattered electrons and other nuclear physics applications.

Acknowledgments:

We acknowledge support from DOE under Topic No. DOE 2016-24b Grant No. DE-SC0015121.

II. Fabrication of a Strip Detector

a) Provide Photolithography Resolution over Larger Area

In order to satisfy the pitch requirements for this strip detector (200 μm wide strips with 25 μm spacing), we installed a used Karl Suss MJB-3 mask aligner with a 365-405 nm 300 W UV Hg-lamp. Photolithography, metallization (50 nm Cr /200 nm Au) and lift-off processes were adjusted to meet diamond strip detector requirements. **Figure 10** shows an example of typical metal pattern on the 48x15x0.5 mm^3 diamond plate.

The second way in which our lithography process was improved involved control of dust and the defects it causes in each metal trace. A 16' x 20' soft-sided Class 1000 clean room was purchased, delivered and assembled and our cleaning, lithography and sputtering equipment moved into the area as shown in **Figure 11**. A significant yield improvement has been noticed with far fewer bare dots and lines in our metal strips that were caused by dust and particulate.

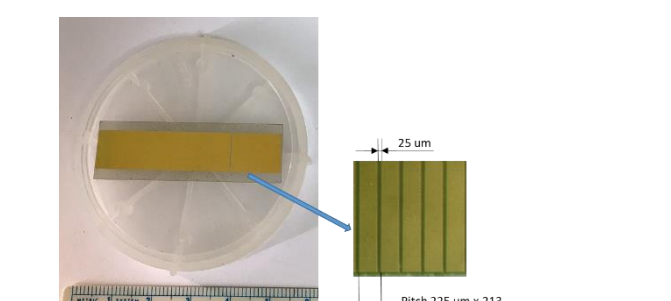


Figure 10. Diamond micro-strip; pCVD plate 15x48x0.5 mm^3 , 25 μm gap between strips, 213 strips, Au/Cr metallization



Figure 11. The photolithography and metallization equipment installed in the new clean room (above), Karl Suss MJB-3 mask aligner with 365-405 nm 300 W UV Hg-lamp (below).

b) Make and Test a Detector

Before cutting and polishing a 48x12 mm plate for the strip detector, Raman analysis was done at each of the 37 locations of the diamond wafer looking for the presence of NV peaks. This data was used to determine which areas to use the cutting of a detector and a number of 10 mm diameter coupons for back-grinding experiments as shown in **Figure 12**.

A diamond plate, 48x12x0.5 mm^3 in size, was cut, polished, metallized and tested. The side of the diamond with the large, single contact was attached to the board with silver-filled UHV epoxy. Each contact strip on the diamond was then Al-wire-bonded to a mating trace on the UHV ceramic board as shown in **Figure 13**. This diamond strip detector was sent to TJNAF for testing and evaluation. While there are no results to report to-date, bench testing is anticipated in the near future and plans are to install this detector, along with 7 Si detectors, in the beam line for operation during the summer 2019.

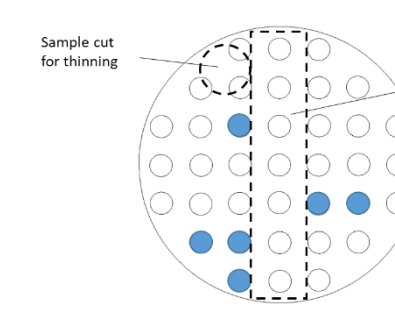


Figure 12. Raman mapping of NV centers in 2" PCD wafer ($\approx 1000 \mu\text{m}$ thick). Blue dots show the presence of NV centers, white - no NV centers. Dashed lines show the locations of plates cut from the wafer

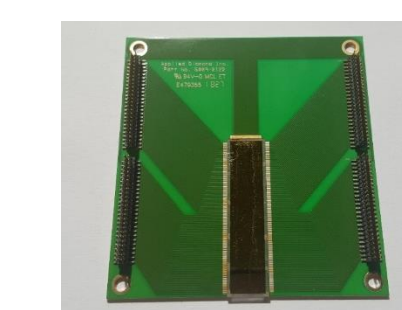


Figure 13. Photo of the roughly 3" square ceramic PCB with 48x12x0.5 mm^3 diamond plate attached and 192 strips connected to 4 Semtec connectors.